MODELLING THE MICROMECHANICAL BEHAVIOUR OF 5-HARNESS SATIN WEAVES OBTAINED BY RTM

A.R. Melro[1*], P. P. Camanho[2], F. M. Andrade Pires[2], S. T. Pinho[3]

[1]*IDMEC - Pólo FEUP, R. Roberto Frias, 4200-465, Porto, Portugal*
[2]*DEMec, Faculdade de Engenharia, Universidade do Porto, R. Roberto Frias, 4200-465, Porto, Portugal*
[3]*Department of Aeronautics, Imperial College London, South Kensington Campus, London, SW7 2AZ, United Kingdom*
**amelro@fe.up.pt*

Keywords: Micromechanics, 5-Harness satin, Continuum damage mechanics, Reduced unit cells.

Abstract
An Offset-reduced Unit Cell (OrUC) model of a 5-harness satin weave is used to characterise damage evolution in this textile composite. Non-linear material models for both yarns and epoxy resin embedding the yarns are applied to the numerical analysis. The epoxy resin is represented by an elasto-plastic with damage constitutive model while the yarns are modelled making use of a transversely isotropic damage model recently proposed. Different loading conditions are applied to the OrUC, allowing for a detailed study of damage initiation and evolution inside the satin weave up until complete failure.

1 Introduction
Thanks to the advance of computational power and numerical tools, micromechanical modelling of composite materials is now giving the first steps. The application of such techniques to textile composites only now is providing the first answers. In this paper, a numerical study on the behaviour of a 5-harness satin weave is performed, making use of an Offset-reduced Unit Cell (OrUC) [1] which strongly reduces the required computations, eliminates repetitive results and allows for a greater resolution on the results. Identical simulations to the ones performed in the past for a full Unit Cell of 5-harness satin [2] are performed and results compared.

For the micromechanical analyses, the satin weave is considered to be assembled by two materials: the reinforcing yarns, and the embedding epoxy. The yarns are considered to be an homogeneous material and are modelled using a recently proposed transverse isotropic damage model [3]. The embedding epoxy matrix is modelled using an elasto-plastic with damage isotropic model [2]. Both constitutive models have been developed under the framework of thermodynamics of irreversible processes and allow for a proper account of the dissipated energy.

2 Offset-reduced Unit Cells

Figure 1a) shows the weaving pattern of a 5-harness satin textile. This represents the Unit Cell corresponding to this particular composite. Figure 1b) exhibits the corresponding Offset-reduced Unit Cell (OrUC). The OrUC can be obtained by taking into account the symmetries existing in the pattern of the woven. In the particular case of a 5-harness satin, different OrUCs can be defined, but the one represented in Figure 1b) is the simplest and easiest to work with.

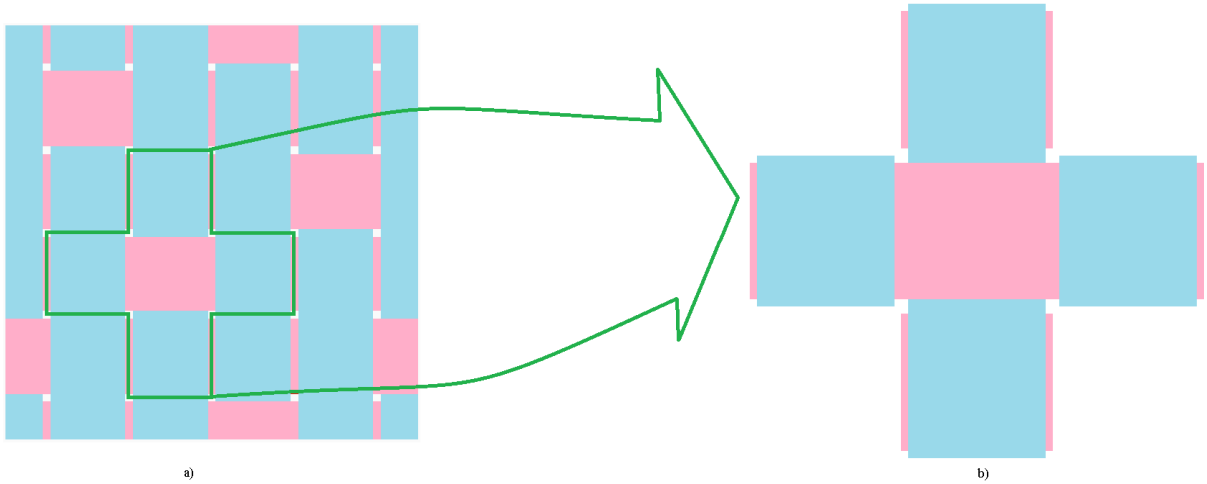

Figure 1. Geometrical representation of a 5-harness satin weave: a) Unit Cell; b) Offset-reduced Unit Cell.

In order to impose material periodicity, periodic boundary conditions (PBCs) were applied to the OrUC, following [1].

3 Constitutive modelling

Each constituent in the OrUC – yarns and matrix – is modelled with an appropriate constitutive model, as detailed next.

3.1 Epoxy matrix

The epoxy matrix is represented by an elasto-plastic with isotropic damage model [2]. The non-linear behaviour of the polymer is captured using a paraboloidal yield criterion [4]. The criterion considers both pressure-dependency of the material as well as different yield strengths in tension and compression. The yield surface is defined by:

$$\Phi(\sigma,\sigma_c,\sigma_t)=6J_2+2I_1(\sigma_c-\sigma_t)-2\sigma_c\sigma_t \tag{2}$$

where J_2 represents the second invariant of the deviatoric stress tensor, I_1 is the first invariant of the stress tensor, and σ_c and σ_t are the yield strengths in compression and tension, respectively. In order to properly account for volumetric deformation, a non-associative flow rule is used, defined as:

$$g=\sigma_{vm}^2+\alpha p^2 \tag{3}$$

where the parameter α represents a material parameter responsible for the correct definition of the volumetric component of the plastic flow [5]. A thermodynamically consistent damage formulation is implemented with a damage activation function formally equal to the yield

criterion, but using compressive and tension ultimate strengths instead of yield strengths. The damage activation function can thus be written as:

$$F_m^d = \frac{3\tilde{J}_2}{X_c X_t} + \frac{\tilde{I}_1 (X_c - X_t)}{X_c X_t} - r_m \leq 0 \tag{4}$$

where the invariants $\tilde{J}_2$ and $\tilde{I}_1$ are determined using the effective stress tensor, and X_c and X_t represent the compressive and tensile strengths of the epoxy. The internal variable r_m is related with the damage variable responsible for degrading the stiffness of the material as damage progresses. This relation is built upon the application of a crack band model [6], which regularises the energy released during damage propagation as a function of the size of the finite elements in the mesh, thus eliminating mesh dependency aspects from the model.

3.2 Yarns

Yarns are regarded as homogenised material, modelled by a transverse isotropic damage model recently proposed by Maimí et al. [3]. The model is capable of predicting both intralaminar and interlaminar damage hanks to its three different damage activation functions:

$$\begin{aligned} F_{L+} &= \frac{E_1}{X_T}\langle \varepsilon_{11} \rangle - r_{L+} \leq 0 \\ F_{L-} &= \frac{E_1}{X_C}\langle \varepsilon_{11} \rangle - r_{L-} \leq 0 \\ F_T &= \sqrt{\left\langle \frac{Y_C - Y_T}{Y_C Y_T}(\tilde{\sigma}_{22} + \tilde{\sigma}_{33}) + \frac{1}{Y_C Y_T}(\tilde{\sigma}_{22} - \tilde{\sigma}_{33})^2 + \frac{\tilde{\sigma}_{12}^2 + \tilde{\sigma}_{13}^2}{S_L^2} \right\rangle} - r_T \leq 0 \end{aligned} \tag{5}$$

where $\tilde{\sigma}_{ij}$ represents the effective stress tensor, Y_C and Y_T are the ultimate transverse strengths of the unidirectional lamina in compression and tension, respectively, X_C and X_T are the ultimate longitudinal strengths of the unidirectional lamina in compression and tension, respectively, S_L is the ultimate longitudinal shear strength, E_1 is the longitudinal Young's modulus and the operator $\langle \bullet \rangle$ is the McCauley operator defined as $\langle x \rangle := (x + |x|)/2$.

The internal variables r_i are defined in such a way as to respect the Kuhn-Tucker loading/unloading conditions. The damage evolution functions were defined implementing a crack band model [6] which accounts for the energy dissipated during the damage propagation and eliminates mesh size dependencies.

The elastic and strength properties for the homogenised yarns were determined by micromechanical analyses performed on a three-dimensional representative volume element (RVE) of the composite material. A batch of five RVEs was generated using a recently proposed algorithm for the generation of random distributions of reinforcements with high fibre volume [7] (Figure 2). Periodic boundary conditions were implemented on the generated RVEs and appropriate loading conditions were applied in order to determine the elastic and strength properties of the homogenised yarns. Table 1 provides the elastic and strength

properties of the constituents – epoxy and carbon fibre – while Table 2 provides the elastic and strength properties of the homogenised material, which will serve as an input to Maimí's constitutive model used in the yarns.

Elastic properties	**AS4 fibres [8]**	**Epoxy [9]**
E_1 (MPa)	225000	3760
E_2 (MPa)	15000	3760
G_{12} (MPa)	15000	1350
G_{23} (MPa)	7000	1350
ν_{12}	0.2	0.39
Strength properties	**AS4 fibres [8]**	**Epoxy [9]**
X_T (MPa)	3350	93
X_C (MPa)	2500	124

Table 1. Elastic and strength properties of constituents of yarns.

Elastic properties	**Yarns**
E_1 (MPa)	138910
E_2 (MPa)	9380
G_{12} (MPa)	5080
ν_{23}	0.350
ν_{12}	0.245
Strength properties	**Yarns**
X_T (MPa)	2056.5
Y_T (MPa)	67.7
Y_C (MPa)	122.5
S_L (MPa)	39.1
S_T (MPa)	47.9

Table 2. Elastic and strength properties of yarns after homogenisation.

4 Numerical analyses

Uniaxial tension, biaxial tension and in-plane shear analyses were performed in order to validate the use of OrUC instead of a full Unit Cell. The fact that there is now a smaller geometry to mesh opens up the possibility for a finer resolution in the stress analysis of the most intricate regions of the satin weave, such as the crimp region. Also worthy of mention is the fact that, given the chosen implicit time integration scheme, convergence is substantially improved with the use of an OrUC over a full UC. Figure 2 shows a detail of the mesh that was used in all analyses performed.

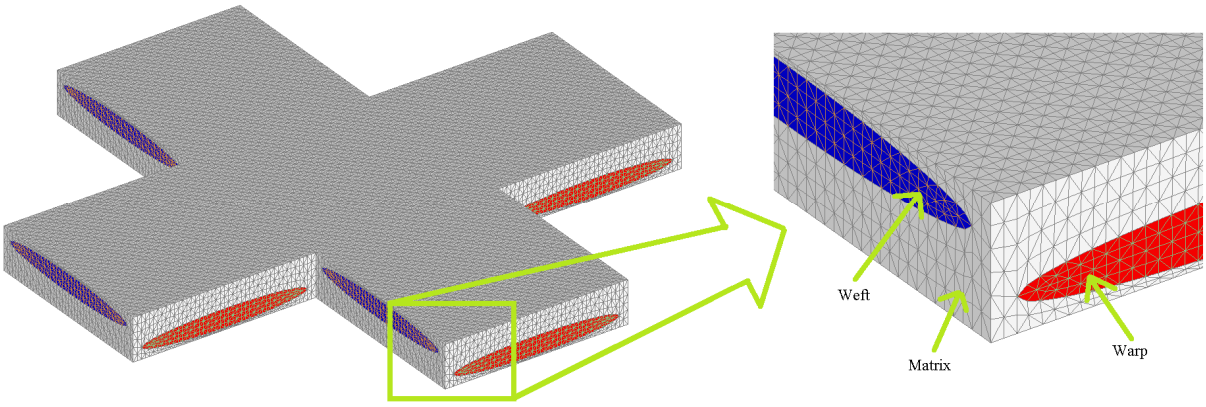

Figure 2. Finite element mesh of the OrUC.

Figure 3 shows the evolution of damage in the 5-harness satin under a uniaxial tension load case. Load is applied along the direction of the warp yarns (horizontal yarns in Figure 3). The first signs of damage are visible close to the crimp area in the warp yarns – Figure 3a). As the load increases, transverse damage propagates not only in the warp yarns, but also the weft yarns – Figure 3b). This leads to a decrease in the stiffness of the material as the fibres in the yarns will progressively lose their lateral support. Transverse damage is caused by the appearance of cracks in the matrix which embeds the fibres in the yarns, and will easily propagate to the matrix embedding the yarns – Figure 3c) – until the crack reaches the surface of the lamina.

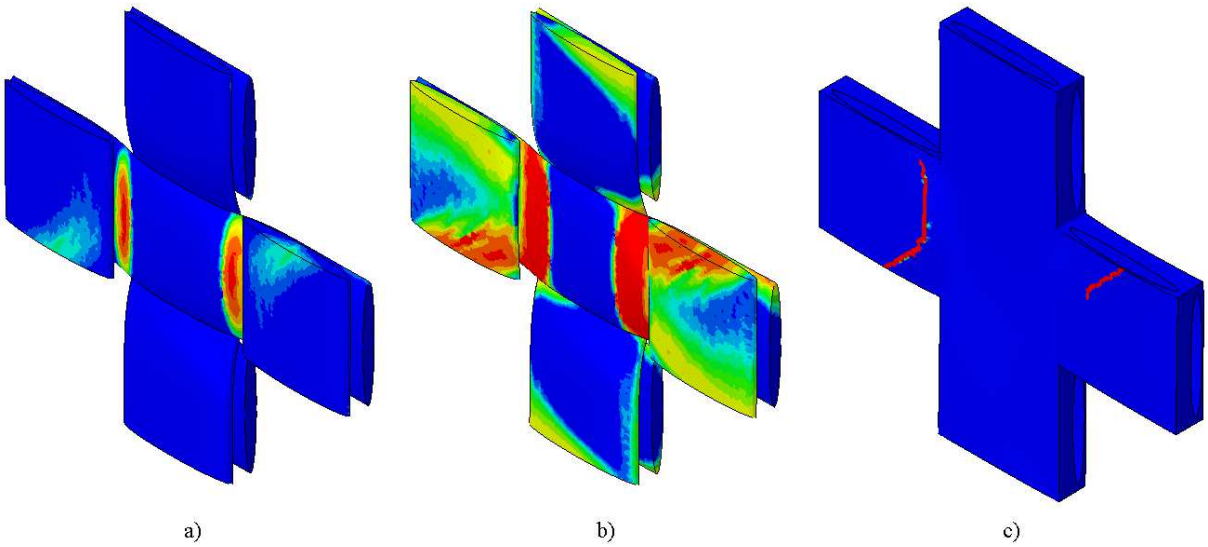

Figure 3. Damage contours for OrUC under uniaxial tension: a) transverse damage with 50% load; b) transverse damage with 100% load; c) surface crack in matrix with 100% load.

Figure 4 shows the occurrence of damage in the 5-harness satin under an in-plane shear load. Under this kind of loading, transverse damage – in the form of transverse cracks in the matrix embedding the fibres in the yarns – will concentrate at the edges of the yarns, both weft and warp yarns. Given the resilience of the matrix under pure shear loads, damage will not propagate swiftly from the yarns to the embedding matrix and, under the applied load, no damage in the matrix was registered.

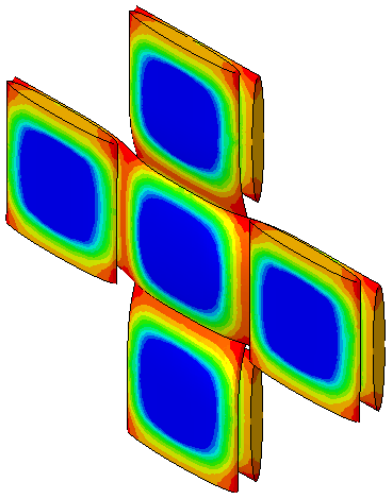

Figure 4. Transverse damage contour for OrUC under in-plane shear load.

Figure 5 represents the evolution of damage under a bi-axial tension load in one lamina of 5-harness satin weave. This load case is extremely similar to a uniaxial load case, except that now transverse damage will be active in equal ways on both warp and weft yarns.

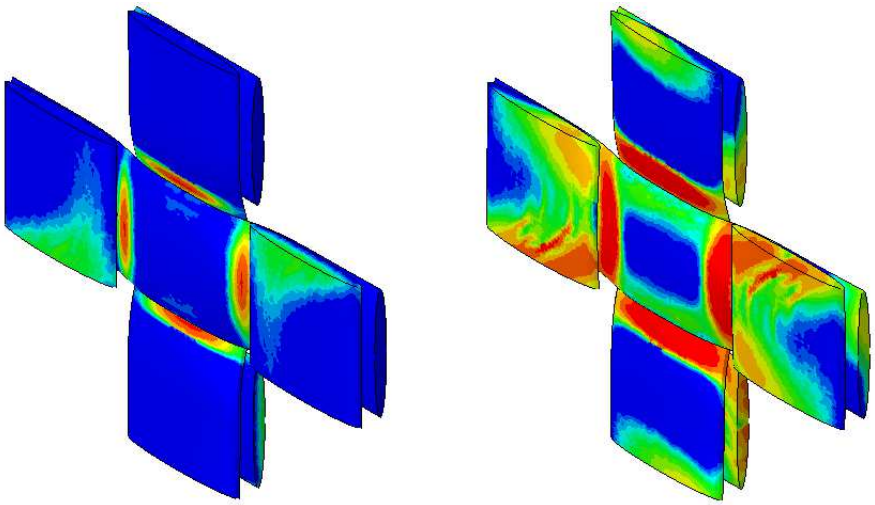

Figure 5. Damage contours for OrUC under bi-axial tension: transverse damage with a) 50% load, b) 100%.

5 Conclusions and future work

The presented work has allowed for the reduction of the size of the cell of a 5-harness satin weave to be analysed by means of micromechanical analyses. This grants the opportunity to acquire with greater resolution the processes involved in damage activation and propagation in textile composites. The developed OrUC greatly reduces the required computational effort and, thanks to periodic boundary conditions, any load combination can be applied to it. In the micromechanical analyses, the yarns are modelled using a transverse isotropic damage model for which the elastic and strength properties were determined using micromechanical analyses. The embedding matrix surrounding the yarns is modelled with an elasto-plastic with isotropic damage model. Uniaxial and biaxial tension, and in-plane shear load cases have been applied and the progression of damage in both constituents has been catalogued.

Next steps in this line of work will involve performing micromechanical analyses on the OrUC under even more different loading schemes which will allow to plot a failure envelope for this particular type of weave. There is also the desire to progress on to the analyses of damage propagation in a laminate configuration, considering the two most extreme situations of lay-up: in-phase and out-of-phase stacking, relatively to the crimp regions.

References

[1] De Carvalho N.V., Pinho S.T., Robinson P. Reducing the domain in the mechanical analysis of periodic structures, with application to woven composites. *Composites Science and Technology*, **71**, pp. 969-979 (2011).

[2] Melro A.R., Camanho P.P., Andrade Pires F.M., Pinho S.T. Numerical simulation of the non-linear deformation of 5-harness satin weaves. *Computational Materials Science*, **61**, pp. 116-126 (2012).

[3] Maimí P., Mayugo J.A., Camanho P.P., A Three-dimensional Damage Model for Transverse Isotropic Composite Laminates. *Journal of Composite Materials*, **42**, pp. 2717-2745 (2008).
[4] Tschoegl N.W. Failure surfaces in principal stress space. *Journal of Polymer Science Part C: Polymer Symposia*, **32**, pp. 239-267 (1971).
[5] Zhang J., Lin Z., Wong A., Kikuchi N., Li V.C., Yee A.F., Nusholtz G.S. Constitutive modelling and material characterization of Polymeric Foams. *Journal of Engineering Materials and Technology, ASME,* **119**, pp. 284-291 (1997).
[6] Bažant Z.P., Oh, B. Crack band theory for fracture of concrete. *Materials and Structures*, **16**, pp. 155-177 (1983).
[7] Melro A.R., Camanho P.P., Pinho S.T. Generation of random distribution of fibres in long-fibre reinforced composites. *Composites Science and Technology*, **68**, pp. 2092-2102.
[8] Soden P., Hinton M., Kaddour A. Lamina properties, lay-up configurations and loading conditions for a range of fibre-reinforced composite laminates. *Composites Science and Technology*, **58**, pp. 1225-1254.
[9] Fiedler B., Hojo M., Ochiai S., Schulte K., Ando M. Failure behaviour of an epoxy matrix under different kinds of static loading. *Composites Science and Technology*, **61**, pp. 1615-1624.